CRYSTAL GROWTH & DESIGN
2006
VOL. 6, NO. 4
1014−1021

Embedding 1,6-Diphenyl-1,2-Dihydronaphthalene (DHN) in 1,4-Distyrylbenzene (DSB): Arene−Arene Interactions in a "Crossed Bis-Diarene"

Yongqiang Sui and Rainer Glaser*

Department of Chemistry, University of Missouri-Columbia, Columbia, Missouri 65211

Received December 13, 2005; Revised Manuscript Received February 28, 2006

Ⓦ **This paper contains enhanced objects available on the Internet at http://pubs.acs.org/crystal.**

ABSTRACT: The $C_{38}H_{32}$ hydrocarbon 1-methyl-1,3,6-triphenyl-7-[(*E*)-2-phenyl-propenyl]-1,2-dihydronaphthalene (**I**) presents a novel framework that combines the functionalities of a 1,6-diarene-substituted 1,2-dihydronaphthalene (DHN) with a 1,4-distyrylbenzene (DSB). The hydrocarbon was synthesized, the crystal structure of (±)-**I** was determined, and a detailed analysis of intermolecular interactions is presented. The crossed bis-diarene **I** has the capability to engage in arene−arene interactions in two nearly orthogonal directions, and various types of arene−arene interactions cooperate in the formation of its lamellar crystal architecture. While the DSB units alternate within both the *R*- and the *S*-substructures, the homochiral substructures feature opposing polarity along the long axes of the DHN-based diarenes, and hence the possibility exists for polar quasiracemic crystals. Importantly, the analysis of arene−arene contacts provides strong evidence that chemical modifications of the arenes attached to the DHN unit are possible without fundamental impediments of the lattice architecture.

Introduction

1,2-Dihydronaphthalenes (DHN) have attracted much interest recently because of their optical properties, and studies were reported on their fluorescence,[1] photochromicity,[2] and photochemistry.[3,4] At the same time, distyrylbenzene (DSB) and its derivatives also have been scrutinized because of their optoelectronic properties,[5−13] and DSB-based dendrimers,[8,14,15] aza-analogues,[16] thin films,[17] polymers,[18] and crystals[19] have been investigated. More efficient syntheses of DHN[20] and DSB[21] have been sought because of this interest in their properties. The $C_{38}H_{32}$ hydrocarbon **I**, 1-methyl-1,3,6-triphenyl-7-(2-phenyl-propenyl)-1,2-dihydronaphthalene, presents a novel framework that combines the functionalities of a diarene-substituted DHN and a substituted DSB (Scheme 1).

Arene−arene interactions are important in the solid state,[22] in solution,[23,24] and in the gas phase;[25,26] the interactions are strong and can be realized in various topologies. We have relied on arene−arene interactions of diarenes of the type Ar−spacer−Ar′ as lateral synthons[27] in the design of polar crystals with layers of parallel beloamphiphiles.[28,29] We explored 1,4-diphenylazines,[30−33] 1,4-diphenylbutadienes,[34] as well as biphenyls.[35] Facile torsion of the arenes along with conformational flexibility of the spacer[36,37] allow for optimization of arene−arene interactions. Hydrocarbon **I** is a crossed bis-diarene with the capability to engage in arene−arene interactions in every direction, and various types of arene−arene interactions cooperate in the formation of its lamellar crystal architecture.

Here, we report a startling one-step synthesis of 1-methyl-1,3,6-triphenyl-7-(2-phenyl-propenyl)-1,2-dihydronaphthalene (**I**), describe its purification and crystallization, and provide a detailed analysis of the crystal structure of (±)-**I**. The proper name of **I** stresses its dihydronaphthalene (**II**) nature, and the DSB framework of **I** is highlighted in red in Scheme 1. The crystal structure of **I** is discussed with reference to structures of the parent biphenyl (**III**, 110 K,[38] 283−303 K[39]), styrene (**IV**, 83 K,[40] 120 K[41]), 1,4-distryrylbenzene (**V**, DSB[42]), and stilbene (**VI**, 295 K[43]). A search of the Cambridge Structure Database suggests that **I** is the first hybrid combining the DHN and DSB frameworks. The analysis of **I** focuses on the interplay between molecular conformation and configuration and intra- and intermolecular arene−arene interactions. The result of the analysis will be an accounting of these arene−arene interactions, and implications for the crystal engineering of polar materials will be discussed.

Scheme 1. Structures of I and of Related Compounds

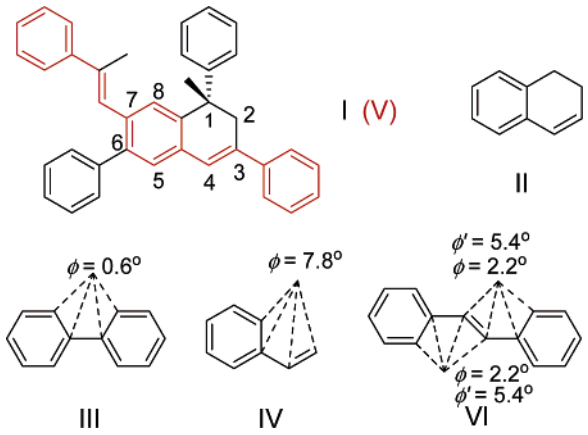

Experimental Section

One-Pot Synthesis. The hydrocarbon **I** was synthesized by the reaction of *β*-methyl-cinnamicaldehyde with diethyl 1-phenylethylphosphonate under modified Horner-Emmons conditions.[44] Forty milligrams (1.64 mmol) of NaH and 3 mL of DME were added to a dry, three-necked flask equipped with a stirrer and a condenser. The flask was immersed in an ice bath and 0.4 mL (1.64 mmol) of diethyl 1-phenylethylphosphonate were injected slowly. The solution was stirred at room temperature for 30 min before the slow addition of 200 mg (1.37 mmol) of *β*-methylcinnamicaldehyde. The solution was heated at reflux for 18 h. After cooling of the two-phase reaction mixture, the flask was filled with water, and the product was extracted with three 20 mL portions of ether. The ethereal extracts were combined and dried

* To whom correspondence should be addressed. E-mail: glaserr@missouri.edu.

10.1021/cg0506626 CCC: $33.50
Published on Web 03/21/2006

Scheme 2. Mechanistic Hypotheses for the Formation of I

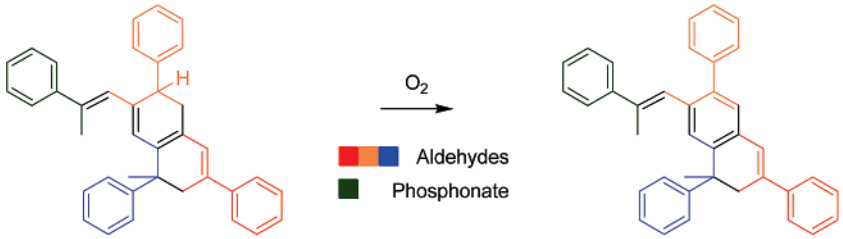

Table 1. Crystal Data and Structure Refinement

empirical formula	$C_{38}H_{32}$
formula weight	488.64
temperature	173(2) K
crystal system, space group	monoclinic, $P2_1/n$
unit cell dimensions	$a = 16.7069(7)$ Å, $\alpha = 90°$ $b = 7.8826(3)$ Å, $\beta = 104.1290(10)°$ $c = 21.2218(8)$ Å, $\gamma = 90°$
volume	2710.23(18) Å^3
Z, calculated density	4, 1.198 Mg/m^3
crystal size	0.35 × 0.35 × 0.25 mm
refinement method	full-matrix least-squares on F^2
goodness-of-fit on F^2	1.035
final R indices [$I > 2\sigma(I)$]	R1 = 0.0445, $\omega R^2 = 0.1047$
R indices (all data)	R1 = 0.0635, $\omega R^2 = 0.1135$

over anhydrous sodium sulfate, and the solvent was removed by rotatory evaporation. The mixtures were purified by gel-permeation chromatography using ethyl acetate and hexane as eluents. The crude product was purified by growing crystals by slow diffusion of hexanes into a ethyl acetate solution (45 mg, 20%).

Spectroscopic Characterization. The identity and purity of **I** was confirmed by ^{1}H and ^{13}C NMR spectroscopy and by mass spectrometry. ^{1}H NMR ($CDCl_3$, 300 MHz, δ in ppm): 1.79 (3H, s), 2.06 (3H, d, J = 1.2 Hz), 2.91 (1H, d, J = 18 Hz), 3.40 (1H, d, J = 18 Hz), 6.66 (1H, s), 6.92 (1H, s), 7.26−7.55 (22H, m). ^{13}C NMR ($CDCl_3$, δ in ppm): 17.3, 27.3, 42.7, 43.3, 76.4, 77.0, 77.5, 123.5, 125.0, 125.2, 125.7, 126.2, 126.9, 127.4, 127.5, 127.8, 128.0, 128.2, 128.4, 128.5, 128.6, 128.7, 129.5, 129.7, 133.1. EI-MS (m/z): 488 (M^+), 489, 490, 486, 411.

X-ray Single-Crystal Structure Determination. Single crystals suitable for X-ray analysis were grown by repeated recrystallization at room temperature. Pertinent crystal data are summarized in Table 1, an *ORTEP* drawing is provided in Figure 1, and details of the crystal structure analysis are reported elsewhere.[45]

Discussion

Mechanistic Hypotheses for the Formation of I. The formation of **I** was discovered serendipitously during the development of a general synthesis for unsymmetrical 1,4-diphenylbutadienes. Instead of the 1:1 coupling of β-methyl-cinnamicaldehyde with diethyl 1-phenylethylphosphonate, the hydrocarbon **I** is formed by the reaction of three molecules of β-methyl-cinnamicaldehyde and one molecule of diethyl 1-phenylethyl-phosphonate. (We also achieved the 1:1 coupling using different reaction conditions.) Scheme 2 shows the scenario that appears most suited to explain the currently known facts. The three aldehydes condense to construct three bonds of ring **A**, the phosphonate connects arene **C**, and air oxidation of the primary condensation product affords the aromatization of the **A** ring.

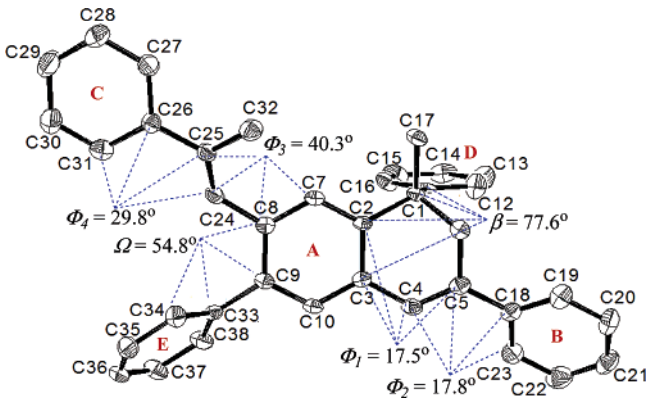

Figure 1. Thermal ellipsoid representation of 1-methyl-1,3,6-triphenyl-7-(2-phenyl-propenyl)-1,2-dihydronaphthalene, (±)-**I**, and naming of arenes **A**−**E**. H atoms are omitted for clarity.

The precise mechanism of the stunning formation of **I** is currently under investigation. The optimization of the ratio between the reactants is nontrivial as this ratio influences not only the formation of **I** but also of other condensation products.

Molecular Characteristics, Lateral Offsets, and Phenyl Twists. DSB prefers *E*-configured C=C double bonds, and the same is true in **I**. There is however a remarkable conformational difference. While DSB itself prefers the anti-conformation with regard to the 1,4-exocyclic bonds of arene **A**,[42] **I** crystallizes in the syn-conformation. The syn-conformation could be adopted to avoid steric interference between the C32 methyl group and arene **E** and/or to optimize intermolecular bonding in the crystal. We recently argued that the syn-conformation is beneficial for intermolecular binding in the biphenyl AMB.[35]

In addition to the adoption of the *syn*-conformation, **I** features a number of more subtle, yet distinguishing characteristics in the phenyl twists and the lateral offsets that describe spacer-connected diarenes.

The phenyl twists can be con- or disrotatory (Scheme 3). Conrotation leads to parallel (if $\Phi_1 = \Phi_2$, $\omega = 0$) or nearly parallel (if $\Phi_1 \neq \Phi_2$, $\omega = |\Phi_1 - \Phi_2|$) arenes with parallel offset (*ParOS*, p) between the best arenes planes ($p = {}^1/_2 l[\sin(\Phi_1) + \sin(\Phi_2)]$), while disrotation leads to a significant torsion ($\omega = \Phi_1 + \Phi_2$). The crystal structures of styrene **IV** are essentially the same with minor differences in the Ph−C_2H_3 torsion (Φ = 7.8° at 83 K,[40] Φ = 6.5° at 120 K[41]), and we discuss the low-T data. The crystal structure of stilbene **VI** features two independent C_i-symmetric molecules ($\Phi_1 = \Phi_2 = \Phi$) with torsion angles Φ = 2.2° and Φ' = 5.4°.[43] While **IV** and **VI** essentially are planar, the torsion angles $\Phi_1 - \Phi_4$ in **I** deviate much more from zero and with different consequences for the stilbenes involving rings **A** and **B** or **A** and **C**, respectively. In the stilbene part of **I** that involves arenes **A** and **B**, the torsions Φ_1 and Φ_2 are disrotatory with $\omega = \Phi_1 + \Phi_2$ = 35.3° (Figure 2). On the other hand, the conrotatory torsions Φ_3 and Φ_4 leave arenes **A** and **C** almost parallel with ω = 10.5°, and the distance between the benzene planes is p = 0.630 Å.

The lateral offset l depends on the angles $\alpha = \angle(C_{ipso}{-}C{=}C)$ and the C=C bond length; $l = d_{C=C}\cos(\alpha)$ or more generally $l = d_{C=C}0.5[\cos(\alpha_1) + \cos(\alpha_2)]$. We use the styrene data as reference; $d_{C8=C7}$ = 1.325 Å, α = 127.07°, and l = 1.051 Å. The two independent molecules of stilbene feature shorter vinyl bonds of 1.264 and 1.307 Å (av. 1.286±0.022 Å), the angles α = 127.47° and α' = 127.09° are about the same, and the lateral

Scheme 3. Lateral Offset and Phenyl Twisting in Diarenes

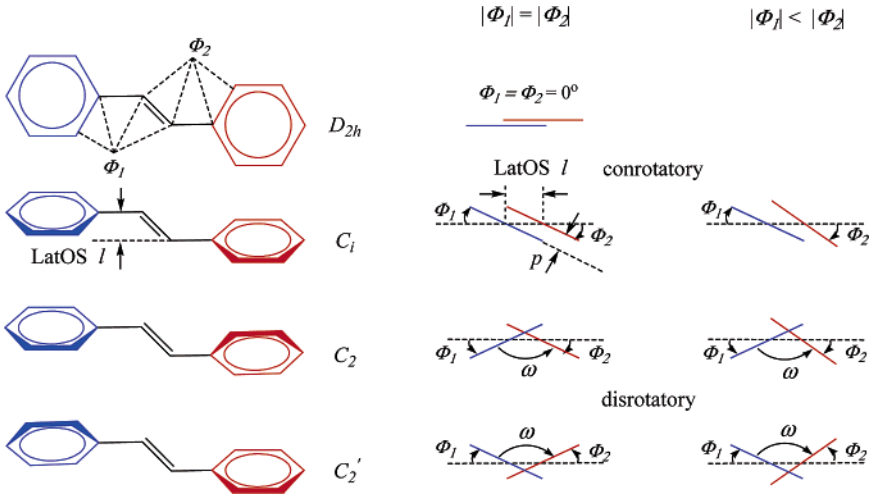

offsets are $l = 1.008$ and $l' = 1.037$ Å. The vinyl bonds in **I** are "normal" ($d_{C4=C5} = 1.339$ Å, $d_{C24=C25} = 1.345$ Å), and the α angles are in line with steric considerations. While the α angles in styrene and stilbene are greater than 127° because of the relative sizes of H and CHR, only α_3 is of comparable size in **I** and α_1, α_2, and α_4 all are just slightly larger than 120°. With the bond lengths about the same and angles equal or smaller, the lateral offsets in **I** become $l_1 = 1.122$ Å and $l_2 = 1.109$ Å, and markedly larger than in **IV** and **VI**.

Lamellar Structure and Woven-Wire Architecture. Molecule **I** has a chiral center (C1), and the crystal is a racemate.[46,47] In Figures 3−6, the *R*- and *S*-enantiomers are shown in green and orange, respectively, and darker color is used in Figure 3 to indicate depth. Figure 3 shows parts of two layers (vertical), and one of these (the left layer in Figure 3) is shown in Figure 4 down the long axes of the molecules. It is evident from Figure 4 that there are no direct stacking interactions because the stacking distance is very long (7.883 Å). Instead, the stacks are bound by bridging interactions provided by the molecules in neighboring stacks. In addition to the two neighbors with the same configuration in the stack, every molecule is surrounded by two *S*- and two *R*-enantiomers in the neighboring stacks because of this double-stack alternation.

Layers are formed by aligning homochiral stacking with double-stack alternation of stacks of *R*- and *S*-enantiomers. This is illustrated in Scheme 4. The top and bottom halves of Scheme 4 show the same molecules, and the perspective is the same as in Figure 4 (top) or in Figure 8 (bottom, the other side of the same layer). The color scheme is as in Figure 4 in that the DSB backbones of the *R*- and *S*-enantiomers are shown in dark green and orange, respectively, and arenes **B** and **C** appear on the layer surface in those colors. But different colors are used for

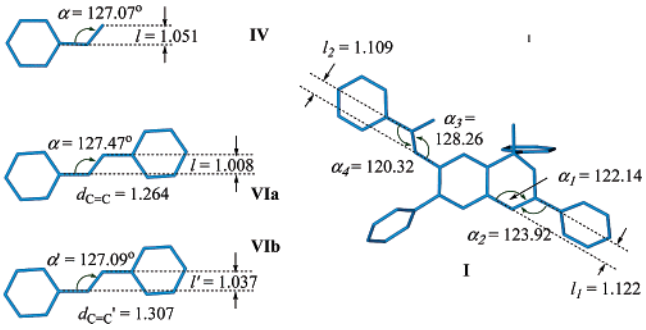

Figure 2. Characteristics of molecules **I**, **IV**, and **VI**. The twist angles Φ_i determine the angle ω between the benzene planes. The lateral offset l and twists Φ_i determine the parallel offset p between the arenes.

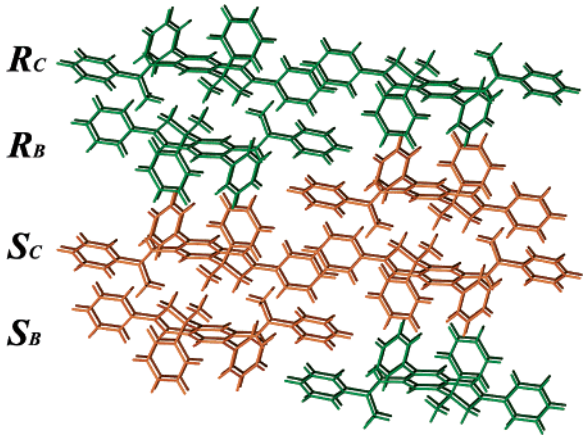

Figure 3. Homochiral stacks of *R*- and *S*-enantiomers (shown in green and orange), respectively, alternate in layers of (±)-**I**. Stacks are perpendicular to the paper plane, and the second layer direction is vertical.

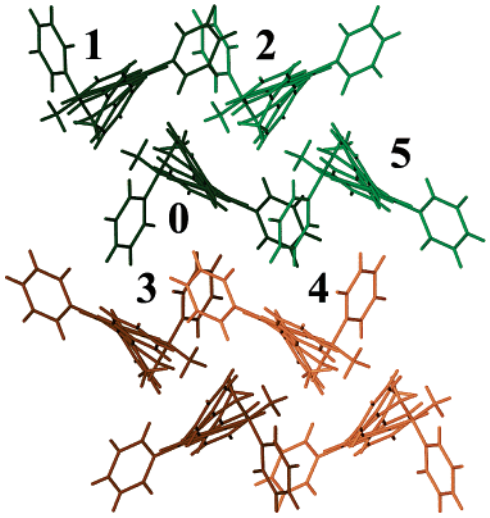

Figure 4. Layer in crystal of (±)-**I** viewed in the direction of the long molecular axes.

Ⓦ A 3D rotatable structure of (±)-**I** is available. Note that the free CHIME plugin is required for the display of the html/pdb files in this paper.

Scheme 4. Layer Pair Binding Topology

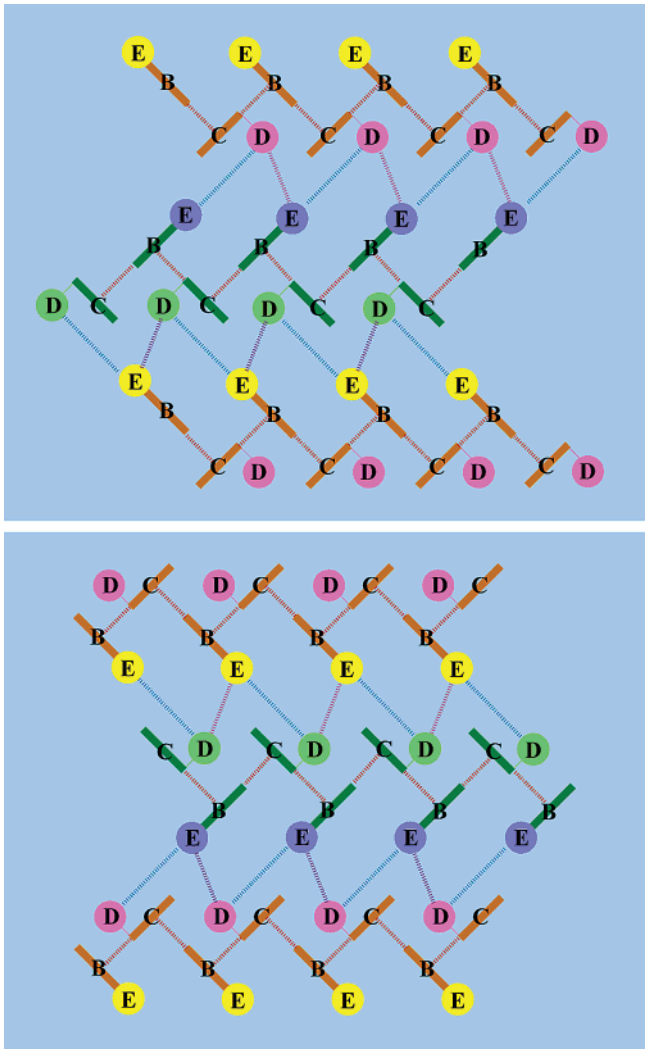

arenes **D** and **E** in Scheme 4 and Figure 8. For *R*-enantiomer, arenes **D** are shown in lime-green and the biphenyl arenes **E** are in orchid-blue, whereas for the *S*-enantiomer, arenes **D** are magenta and biphenyl arenes **E** are yellow.

Scheme 4 shows the pair binding topology in a half-layer; that is, for every molecule are shown only arenes **B** and **D** or arenes **C** and **E**, respectively. Pairs 1 and 2 are enantiomer associations,[48] and their (identical) interactions are indicated as dashed red lines in Scheme 4. Pairs 3 and 4 are diastereomers, and their (different) interactions are indicated as dashed lines in turquoise and plum. Consequently, different spacings occur between the homochiral domains and between stacks of opposite chirality.

Arene−Arene Preferences and Molecular Orientation. The pair interactions involve arenes **B**−**E**, not arenes **A**, and the interactions involve either arenes **B** and **C** or arenes **D** and **E**. The long axes of the DSB units are more or less perpendicular to the layer surfaces, and the two molecules in every pair are oriented in opposite directions! For a molecule with a given **B**-to-**C** direction (e.g., "0" in Figure 4), *all* of its next neighbors in neighboring stacks (e.g., "1"−"4") are oriented in the opposite direction (see Scheme 4). The homochiral double stacks together with this alternation of the orientations results in the four-stack repeating unit $\{R_C\ R_B\ S_C\ S_B\}$. In contrast, the **D**-to-**E** directions point to the same end of the stack in the two stacks of every homochiral double-stack, and the **D**-to-**E** directions alternate between the homochiral double-stacks. While the DSB units alternate within both the *R*- and *S*-substructures, the homochiral substructures feature opposing polarity along the long axes of the DHN-based diarenes.

Modi of Intermolecular Pair Binding. Pairs 1−4 are shown in Figure 5 with the perspective of Figures 3 and 4 on the left and right, respectively. In Figure 6, the arene−arene contacts in pairs 3 and 4 are shown again with space-filling models.

Pair 1 is a fancy double T-contact of the (ff|ee) type, that is, arenes **B** and **C** of the DSB moiety function as faces and arenes **C** and **B** of the neighboring molecule's DSB moiety function as edges in two lateral arene−arene T-contacts. Because of the opposite orientation of next neighbors with regard to the given **B**-to-**C** direction, one molecule's **B** arene interacts with the equal-configuration neighbor's **C** arene and vice versa. The DSB moiety functions just like a "spacer-connected diarene" with arene **A** being part of the spacer. The **B** and **C** rings of one *R*-enantiomer (e.g., "1") function as faces, and the **C** and **B** rings of the other *R*-enantiomer function as edges (e.g., "0"). Pair 2 is the enantiomer of pair 1 and the (ff| part is now provided by that *R*-enantiomer that served as the |ee) part in pair 1 (e.g., "0") and another *R*-enantiomer serves as the (ee| part (e.g., "2")).

The bonding of pairs 3 and 4 involves arenes **D** and **E**, and arenes **B** and **C** do not play a role. Arenes **D** and **E** engage in double T-contacts of the (ef|fe) type in both pairs. The arenes **D** are faces in pair 3, and they are edges in pair 4 and vice versa for arenes **E**.

There is one major difference between pairs 1 and 2, on one hand, and pairs 3 and 4, on the other. Of course, in pairs 1 and 2 the interactions between the arene pairs are possible *only* laterally. The arenes **D** and **E** also provide for lateral interaction with the (**D**, **E**) interactions. However, there now exists the additional possibility for (**D**, **D**) or (**E**, **E**) interactions, and Figure 6 (left column) helps to examine whether this possibility is realized. As can be seen, pair 3 features essentially coplanar (**D**, **D**) pairs, and pair 4 features very much offset and nearly coplanar (**E**, **E**) interactions. These geometries suggest that the (**D**, **D**) and (**E**, **E**) contacts are hardly binding. This recognition at first was somewhat of a surprise. The (**D**, **E**) contacts in pairs 3 and 4 should be more or less invariant to rotations of the **D** or **E** arenes, respectively, because they are edges of T-contacts, and there are no compelling intramolecular reasons to hinder any such conformation adjustments. Since much could be gained from minor conformational changes, why do they not occur? Our analysis reveals two plausible reasons: one is due to arene−arene triple interactions involving arenes **A**, and the other relates to an indirect stacking interaction.

Arene A Involvement, Indirect Intrastack Interactions, and "Arene−Biphenyl" Interactions. To a first approximation, we have described the arene−arene interactions in pairs 3 and 4 by way of pair interactions between arenes **D** and **E**. A more complete understanding also requires the consideration of arenes **A**. Instead of two (**D**, **E**)-pair interactions, there actually are two (**D**, **E**, **A**)-triple interactions and one of these (**D**, **E**, **A**)-triples is shown for each pair in spacefill in the right column of Figure 6.

In pair 3, **D** interacts with **A** by way of a T_H-contact, e.g., by pointing the C_{meta}−H bond toward the center of **A**'s π-face. In the T_H-contact, as in any T-contact, one arene serves as face and the other arene's plane is more or less perpendicular. While most T-contacts involve the interaction of an arene edge with an arene face, e.g., an arene−π-interaction with *two* arene hydrogen atoms, a T_H-contact involves an arrangement in which one arene C−H bond is oriented toward an arene face, e.g., an

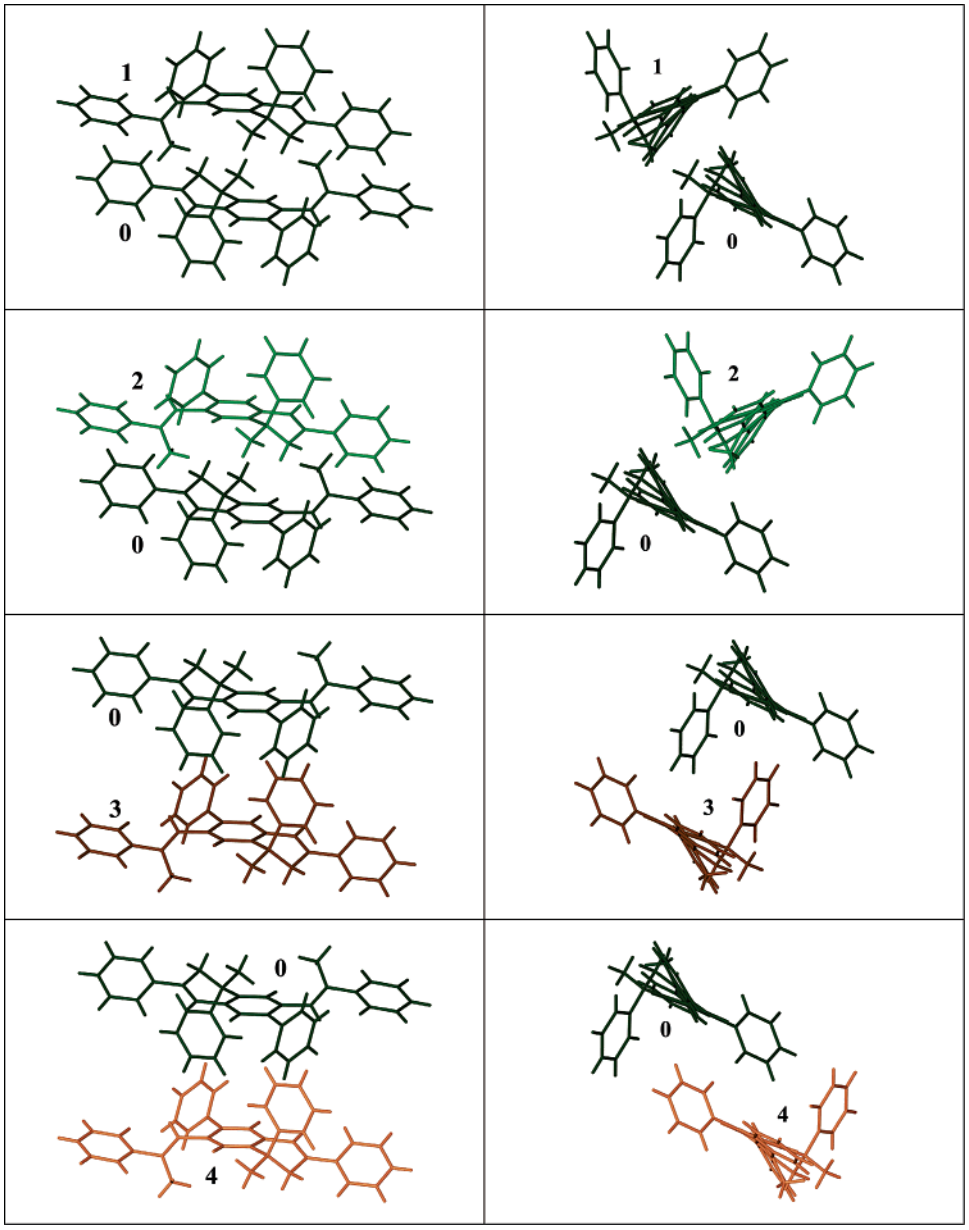

Figure 5. Pair interactions in crystals of (±)-**I**. The *R*-enantiomer (green) is surrounded by two *R*- and two *S*-enantiomers. Perspectives in the left and right columns are as in Figures 3 and 4, respectively. Pairs 1 and 2 are enantiomeric dimers of the same enantiomer while pairs 3 and 4 are diastereoisomeric dimers of opposite enantiomers.

Ⓦ 3D rotatable structures Ⓦ pair 1, Ⓦ pair 2, Ⓦ pair 3, and Ⓦ pair 4 are available.

arene−π-interaction with *one* arene hydrogen atom. In pair 4, arene **E** engages in an additional contact with an arene **A**, and this contact is an e(**E**)f(**A**)-contact that involves the CH_{meta}−CH_{para} edge of **E**.

Direct stacking interactions occur, for example, in stacks of arenes[49] or graphene sheets.[50] Direct stacking implies that the translation in the stacking direction is small enough so that any fragment of one molecule will be close enough *to the same fragment* in the next molecule. While the stacking distance in the homochiral columns prevents *direct* stacking interactions, there are *indirect* intrastack arene−arene T-contacts between **D** and **E** arenes in pair 5, and these are illustrated in Figure 7. As with pair 3, arene **D** engages in an additional T_H-contact interaction with arene **A**, but their roles are reversed. This T_H-contact is picture-perfect: the C_{para}−H bond of **A** is directed toward the center of **D**'s π-face, the long axis of **A** is perpendicular to the **D** plane, and the cross-section between the **A** and **D** planes contains a para-related CH group of **D**.

In pairs 3 and 5, the biphenyl **A**-**E** of one molecule interacts with arene **D** of the other. The biphenyl acts as a double-face in both cases, while the role of **D** varies. Arene **D** serves as an edge and a CH-donor in pair 3 and does so using just two CH-groups. In pair 5, arene **D** serves as a face and an edge. It is important to note that all these interactions involve CH-groups that are closer to the center of the molecule ("inside"): in pair 3 the inside-meta and the para-positions are used and in pair 5 the inside-ortho and inside-meta positions are engaged.

Interlayer Binding. The intralayer binding topology of Scheme 4 is illustrated by the space-filling model in Figure 8. The (**B**, **C**) T-contacts in pairs 1 and 2 are nicely seen to form infinite chains in which every arene serves as a face in one and as an edge in the next T-contact. (**B**, **C**)-ridges are build

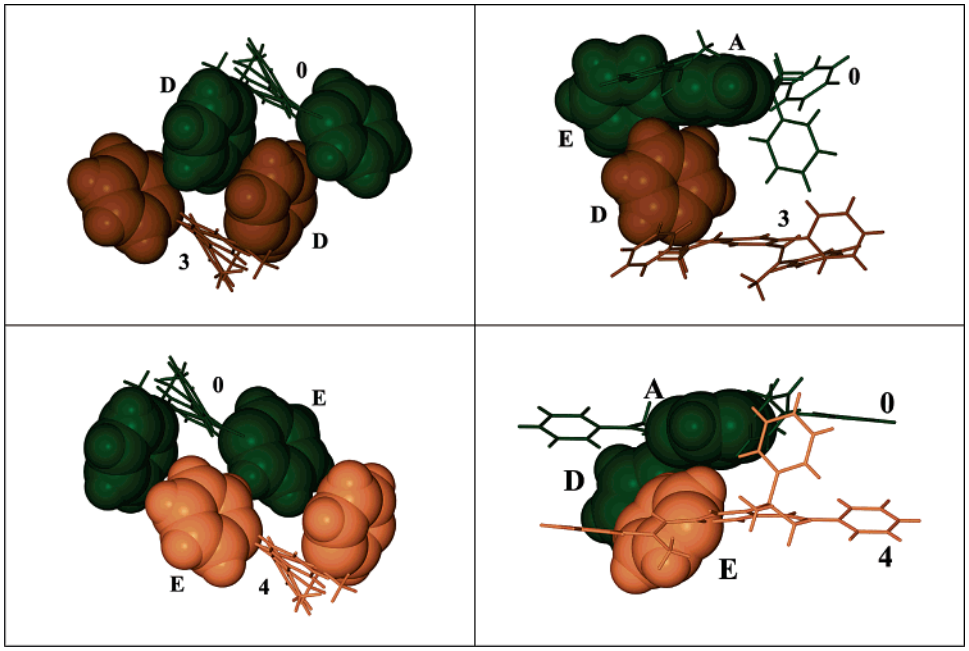

Figure 6. Space-filling models of pairs 3 and 4. The models on the left show (**D**, **E**) pairs, they are oriented just like the side views in Figure 5, and they show that arenes **D** are coplanar in pair 3 and that arenes **E** also are nearly in the same plane in pair 4. The models on the right show one of two identical (**A**, **D**, **E**)-triples involving pair 3 and pair 4.

Ⓦ 3D rotatable space-filling models of Ⓦ pair 3 and Ⓦ pair 4 and of the (**A**, **D**, **E**)-triples with Ⓦ pair 3 and Ⓦ pair 4 are available.

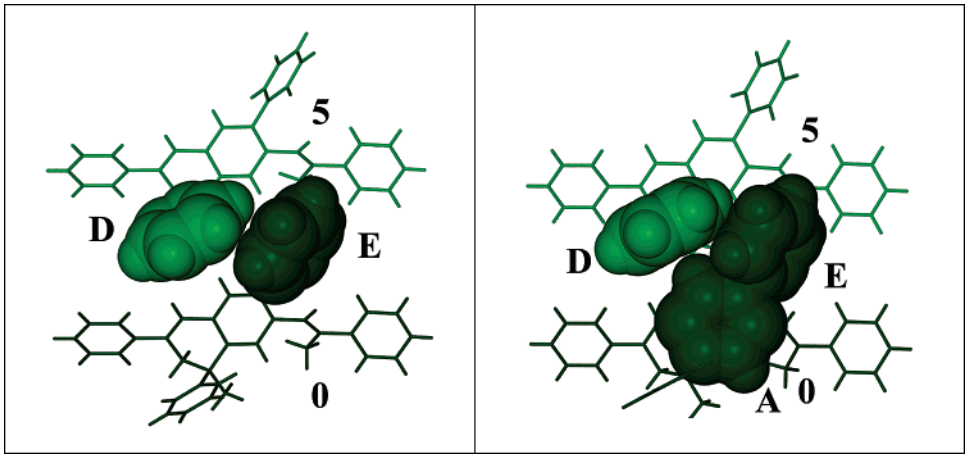

Figure 7. The only significant intrastack interaction is an "arene−biphenyl" interaction. This interaction involves one T-contact between arenes **D** and **E** as well as one T_H-contact between the same arene **D** and the arene **A** attached to arene **E.** Each molecule is involved in two such (**A**, **D**, **E**)-triple interactions. The image on the left emphasizes the (**D**, **E**) T-contact, and the image on the right shows the (**A**, **D**, **E**) triple.

Ⓦ 3D rotatable structures of the Ⓦ (**D**, **E**) T-contact and the Ⓦ (**A**, **D**, **E**) triple are available.

alternatively with *R*- or *S*-enantiomers, and there are valleys of two kinds between the (**B**, **C**)-ridges: The valley floors feature either arenes (*S*)-**D** (magenta) and (*R*)-**E** (orchid) or (*R*)-**D** (lime) and (*S*)-**E** (yellow), respectively. The walls of the valleys are lined with edges and faces of arenes **B** and **C**.

The valleys are occupied by arenes **B′** and **C′** of the next layer. One of the **B′** and one of the **C′** arenes of the *R*-enantiomers in the next layer are shown in blue in Figure 8. The layers are stacked with nothing but a small lateral offset from layer to layer (Figure 3), and thus the **C′** arene dives the deepest into the surface and engages in *four* interlayer arene−arene interactions: in two lateral T-contacts with one (orange) **C** and one (dark-green) **B** arene serving as face in both, in one lateral T-contact with another (orange) **C** arene serving as edge, and in one longitudinal arene−arene T_H-contact involving the **C′** arene and one (yellow) **D** arene. Similarly, each **B′** arene engages in *four* interlayer arene−arene interactions: as face in two interlayer, lateral ff-contacts with (dark green) **B** arenes, as edge in one interlayer T-contact with one (dark green) **C** arene, and one interlayer, longitudinal arene−arene T_H-contact with a (lime green) **E** arene. The interlayer interaction of the *S*-enantiomer involves the enantiomeric interactions.

Accounting of Arene−Arene Interactions by Number, Type, and Discrimination. The results of the analysis of arene−arene interactions is summarized in Table 2. All triple interactions are treated as two pairs, and the entries refer to the intralayer binding of one half-layer and its interlayer binding. Every (**B**, **C**), (**D**, **E**), (**A**, **D**), and (**A**, **E**) pair interactions appear as an entry in the rows of both arenes and with the factor $^1/_2$. The factor $^1/_2$ results as the product of one factor of $^1/_2$ to avoid double counting, the factor 2 because this interaction occurs twice for each molecule, and another factor of $^1/_2$ to count only

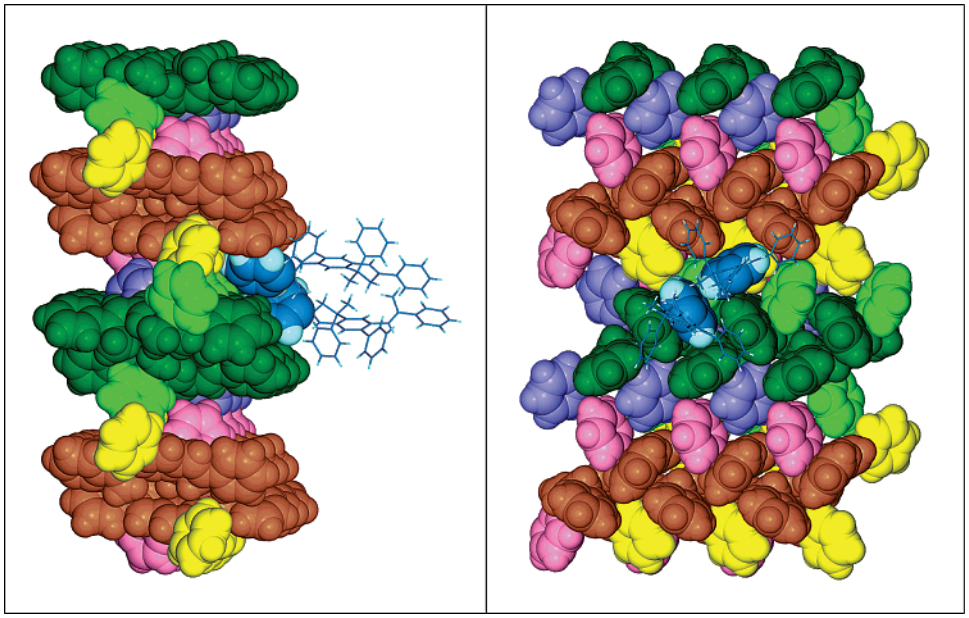

Figure 8. The interlayer interaction features a variety of arene−arene interactions between arenes **B** and **C** of one layer with arenes **B′** and **C′** of the next layer as well as involvement of arenes **D** and **E** in interactions with arenes **B′** and **C′**.

Table 2. Arene−Arene Interactions Per Half-Layer

Ar	Intralayer					Interlayer
	Interstack				Intrastack	
	Pair 1	Pair 2	Pair 3	Pair 4	Pair 5	
B	½ f(B)e(C)	½ e(B)f(C)				½ e(B')f(C) ½ f(B')f(B) ½ f(B')f(B) ½ h(B')f(E)
C	½ f(B)e(C)	½ e(B)f(C)				½ f(C')e(B) ½ f(C')e(C) ½ e(C')f(C) ½ h(C')f(D)
D	-	-	½ e(D)f(E) ½ h(D)f(A)	½ f(D)e(E)	½ e(D)f(E) ½ f(D)h(A)	½ h(C')f(D)
E	-	-	½ e(D)f(E)	½ f(D)e(E) ½ f(A)e(E)	½ e(D)f(E)	½ h(B')f(E)
A			½ h(D)f(A)	½ f(A)e(E)	½ f(D)h(A)	

the half-layer contributions. The cell shading indicates blocks of interactions that depend on various sets of intramolecular characteristics. Shaded red are interactions that depend mostly on the syn-conformation, phenyl torsions Φ_i, and offsets *p* and *l*. Shaded yellow are interactions that depend mostly on torsions Ω and β. Shaded green are interactions that depend on all those variables. The complexity is enormous and tractable, if at all, only by simulation.

Despite all this complexity, the crystal architecture can be readily conceptualized based on an accounting of intermolecular interactions, and in Table 3 an accounting is presented of the numbers of engagements of arenes **A**−**E** in arene−arene interactions, of their types, and of the frequency and the preference of each arene's function in the arene−arene contacts. The analysis allows for the following observations.

(1) Clearly, (**B**, **C**) interactions contribute most to the binding. Both of these arenes are involved in *six* arene−arene interactions (n_{tot} = 6), e.g., one more contact that one might reasonably have expected!

(2) (**B**, **C**) interactions contribute more to interlayer binding (L_{tot} = 2) than to interlayer binding (I_{tot} = 4); r_{LI} = 0.5.

Table 3. Numbers of Engagement and Preferred Functions

		no. of engagements				preferred function	
Ar		edge X_e	face X_f	C−H X_h	total X_{tot}	$f_X = X_f/X_e$ ($f_X = X_f/X_{tot}$)	L_{tot}/I_{tot} r_{LI}
B	intralayer (*L*)	1	1	0	2	1.0 (0.5)	
	interlayer (*I*)	1	2	1	4	2.0 (0.5)	
	all (*n*)	2	3	1	6	1.5 (0.5)	0.5
C	intralayer (*L*)	1	1	0	2	1.0 (0.5)	
	interlayer (*I*)	1	2	1	4	2.0 (0.5)	
	all (*n*)	2	3	1	6	1.5 (0.5)	0.5
D	intralayer (*L*)	2	2	1	5	1.0 (0.4)	
	interlayer (*I*)	0	1	0	1	undefined	
	all (*n*)	2	3	1	6	1.5 (0.5)	5.0
E	intralayer (*L*)	2	2	0	4	1.0 (0.5)	
	interlayer (*I*)	0	1	0	1	undefined	
	all (*n*)	2	3	0	5	1.5 (0.6)	4.0

(3) Arenes **B** and **C** both serves as edge twice (n_e = 2), as face three times (n_f = 3), and once as H-donor (n_h = 1).

(4) All intralayer (**B**, **C**) interactions are mixed. The number of mixed (**B**, **C**) interlayer interactions is half the number of pure interlayer interactions involving two **B** or **C** arenes.

(5) Arenes **E** arenes are "underutilized" in that they engage only in five arene−arene interactions (n_{tot}= 5), e.g., one *less* than **A**−**D**.

(6) Arenes **D** and **E** contribute more to intralayer binding (L_{tot} is 5 and 4, respectively) than to interlayer binding (I_{tot} = 1); r_{LI} values are 5 and 4, respectively.

(7) While arenes **B**, **C**, and **D** agree in number and type of contacts, arene **E** differs because it does not serve any h-function.

(8) All (**D**, **E**) interactions are mixed.

Conclusion

We have synthesized the hydrocarbon $C_{38}H_{32}$ in a one-pot reaction from simple starting materials and in comparatively high yield. The reaction forms racemic **I**, and single crystals contain the racemate (±)-**I**.

While the orientations of the DSB moieties alternate within both the *R*- and the *S*-substructures, the homochiral substructures feature opposing polarity along the long axes of the DHN-based

diarenes. Hence, the possibility exists for the achievement of polar single crystals by rational design. Englert[51,52] and Wheeler[53,54] described quasiracemic crystals of organic and organometallic compounds, respectively. Quasiracemates are 1:1-cocrystals of (*R*)-**1** and (*S*)-**2** that crystallize like (±)-**1** or (±)-**2**, and the components usually feature modest changes in constitution as the result of functional group replacement (Br vs Cl,[53] O vs NH,[53] CH_3 vs NO_2[54]) or because of ligand replacement (CN^- vs NO_2^-,[51] collidine vs. lutidine[52]).

The results of the deep analysis of the arene−arene contacts in (±)-**I** strongly suggest that chemical modifications of arenes **A** and **E** should be possible without introducing any fundamental and/or significant impediments to fit the lattice architecture of (±)-**I**. The arenes **E** are not engaged to the fullest possible extent in arene−arene interactions, and arene **E** should be amenable to chemical modification because only its (inside) *o*,*m*- and *m*,*p*-edges are engaged in arene−arenes interactions, while the (outside) *o*′- and *m*′-positions are not. Also tempting, of course, is a chemical modification of arene **A** at C7 as a strategy to quasiracemic polar materials for electrooptical applications.

Acknowledgment. This work was supported by the MU Research Board (RB #2358). Dr. Len Barbour kindly provided a copy of the program *X-Seed*.

References

(1) Autrey, D.; Arp, Z.; Choo, J.; Laane, J. *J. Chem. Phys.* **2003**, *119*, 2557−2568.
(2) Gorner, H.; Mrozek, T.; Daub J. *Chem. Eur. J.* **2002**, *8*, 4008−4016.
(3) Laarhoven, W. H.; Lijten, F. A. T.; Smits, J. M. M. *J. Org. Chem.* **1985**, *50*, 3208−3209.
(4) Woning, J.; Lijten, F. A. T.; Laarhoven, W. H. *J. Org. Chem*. **1991**, *56*, 2427−2435.
(5) Bartholomew, G. P.; Bazan, G. C. *J. Am. Chem. Soc*. **2002**, *124*, 5183−5196.
(6) Bartholomew, G. P.; Bazan, G. C.; Bu, X.; Lachicotte, R. J. *Chem. Mater*. **2000**, *12*, 1422−1430.
(7) Cheng, G.; Xie, Z.; Zhang, Y.; Xia, H.; Ma, Y.; Liu, S. *Semicond. Sci. Technol*. **2005**, *20*, 23−25.
(8) Luo, F.-T.; Tao, Y.-T.; Ko, S.-L.; Chuen, C.-H.; Chen, H. *J. Mater. Chem*. **2002**, *12*, 47−52.
(9) Grozema, F. C.; Telesca, R.; Snijders, J. G.; Siebbeles, L. D. A. *J. Chem. Phys.* **2003**, *118*, 9441−9446.
(10) Hong, J. W.; Woo, H. Y.; Liu, B.; Bazan, G. C. *J. Am. Chem. Soc*. **2005**, *127*, 7435−7443.
(11) Leng, W.; Grunden, J.; Bartholomew, G. P.; Bazan, G. C.; Kelley, A. M. *J. Phys. Chem. A* **2004**, *108*, 10050−10059.
(12) Lupton, J. M.; Samuel, I. D. W.; Burn, P. L.; Mukamel, S. *J. Phys. Chem. B* **2002**, *106*, 7647−7653.
(13) Pond, S. J. K.; Rumi, M.; Levin, M. D.; Parker, T. C.; Beljonne, D.; Day, M. W.; Bredas, J.-L.; Marder, S. R.; Perry, J. W. *J. Phys. Chem. A* **2002**, *106*, 11470−11480.
(14) Ma, D.; Lupton, J. M.; Samuel, I. D. W.; Lo, S.-C.; Burn, P. L. *Appl. Phys. Lett*. **2002**, *81*, 2285−2287.
(15) Wang, Y.; Ranasinghe, M. I.; Goodson, T. *J. Am. Chem. Soc*. **2003**, *125*, 9562−9563.
(16) Marri, E.; Galiazzo, G.; Mazzucato, U.; Spalletti, A. *Chem. Phys*. **2005**, *312*, 205−211.
(17) Ni, J. P.; Ueda, Y.; Hanada, T.; Takada, N.; Ichino, Y.; Yoshida, Y.; Tanigaki, N.; Yase, K.; Wang, D. K.; Wang, F. S. *J. Appl. Phys*. **1999**, *86*, 6150−6154.
(18) Sarker, A. M.; Kaneko, Y.; Lahti, P. M.; Karasz, F. E. *J. Phys. Chem. A* **2003**, *107*, 6533−6537.
(19) Xie, Z.; Yang, B.; Cheng, G.; Liu, L.; He, F.; Shen, F.; Ma, Y.; Liu, S. *Chem. Mater*. **2005**, *17*, 1287−1289.
(20) Maeda, K.; Farrington, E. J.; Galardon, E.; John, B. D.; Brown, J. M. *Adv. Synth. Catal*. **2002**, *344*, 104−109.
(21) Wong, M. S.; Samoc, M.; Samoc, A.; Luther-Davies, B.; Humphrey, M. G. *J. Mater. Chem*. **1998**, *8*, 2005−2009.
(22) Williams, J. A. *Acc. Chem. Res.* **1993**, *26*, 593−598.
(23) Gung, B. W.; Xue, X.; Reich, H. J. *J. Org. Chem.* **2005**, *70*, 3641−3644.
(24) Gung, B. W.; Patel, M.; Xue, X. *J. Org. Chem.* **2005**, *70*, 10532−10537.
(25) Engkvist, O.; Hobza, P.; Selzle, H. L.; Schlag, E. W. *J. Chem. Phys.* **1999**, *110*, 5758−5762.
(26) Reyes, A.; Tlenkopatchev, M. A.; Fomina, L.; Guadarrama, P.; Fomine, S. *J. Phys. Chem. A* **2003,** *107*, 7027−7031.
(27) Lewis, M.; Wu, Z.; Glaser, R. Arene-Arene Double T-Contacts. Lateral Synthons in the Engineering of Highly Anisotropic Organic Crystals, In *Anisotropic Organic Materials − Approaches to Polar Order*; Glaser, R., Kaszynski, P., Eds.; ACS Symposium Series, Vol. 798; American Chemical Society: Washington, D. C., 2001; Chapter 7; pp 97−111.
(28) Glaser, R.; Knotts, N.; Wu, H. *Chemtracts* **2003**, *16*, 443−452.
(29) Glaser, R. *Acc. Chem. Res*., manuscript submitted.
(30) Chen, G. S.; Wilbur, J. K.; Barnes, C. L.; Glaser, R. *Perkin Trans. 2* **1995**, 2311−2317.
(31) Lewis, M.; Barnes, C.; Glaser, R. *Acta Crystallogr. C* **2000**, *56*, 393−396.
(32) Lewis, M.; Barnes, C. L.; Glaser, R. *J. Chem. Crystallogr*. **2000**, *30*, 489−496.
(33) Glaser, R.; Knotts, N.; Yu, P.; Li, L.; Chandrasekhar, M.; Martin, C.; Barnes, C. L. *Dalton Trans.* **2006**, in press.
(34) Glaser, R.; Dendi, L. R.; Knotts, N.; Barnes, C. L. *Cryst. Growth Des*. **2003**, *3*, 291−300.
(35) Glaser, R.; Knotts, N.; Wu, Z.; Barnes, C. *Cryst. Growth Des.* **2006**, *6*, 235−240.
(36) Glaser, R.; Chen, G. S. *J. Comput. Chem*. **1998**, *19*, 1130−1140.
(37) Sauro, V. A.; Workentin, M. S. *J. Org. Chem*. **2001**, *66*, 831−838.
(38) BIPHEN03: Carbonneau, G. P.; Delugeard, Y. *Acta Crystallogr. B* **1976**, *32*, 1420−1423.
(39) BIPHEN04: Charbonneau, G. P.; Delugeard, Y. *Acta Crystallogr. B* **1977**, *33*, 1586−1588.
(40) ZZZTKA01: Yasuda, N.; Uekusa, H.; Ohashi, Y. *Acta Crystallogr. E* **2001**, *57*, o1189−o1190.
(41) ZZZTKA02: Bond, A. D.; Davies, J. E. *Acta Crystallogr. E* **2001**, *57*, o1191−o1193.
(42) Wu, C. C.; DeLong, M. C.; Vardeny, Z. V.; Ferraris, J. P. *Synth. Met*. **2003**, *137*, 939−941.
(43) Vartanyan, R. S.; Gyul'budagyan, A. L.; Karapetyan, A. A.; Struchkov, Y. T. *Arm. Khim. Zh*. **1986**, *39*, 603−608.
(44) Donkor, I. O.; Huang, T. L.; Tao, B.; Rattendi, D.; Lane, S.; Vargas, M.; Goldberg, B.; Bacchi, C. *J. Med. Chem.* **2003**, *46*, 1041−1048.
(45) Sui, Y.; Barnes, C. L.; Glaser, R. *Acta Crystallogr. C* **2006**, *62*, 98−100.
(46) Jacques, J.; Collet, A.; Wilen, S. H. *Enantiomers, Racemates and Resolutions*; John Wiley: New York, 1981.
(47) Brock, C. P.; Schweizer, W. B.; Dunitz, J. D. *J. Am. Chem. Soc.* **1991**, *113*, 9811−9820.
(48) Marthi, K. *Models Chem.* **1995**, *132*, 435−439.
(49) Tauer, T. P.; Sherrill, C. D. *J. Phys. Chem. A* **2005**, *109*, 10475−10478.
(50) Hashimoto, A.; Suenaga, K.; Urita, K.; Shimada, T.; Sugai, T.; Bandow, S.; Shinohara, H.; Iijima, S. *Phys. Rev. Lett.* **2005**, *94*, 045504/1−045504/4.
(51) Englert, U.; Härter, R.; Hu, C.; Kalf, I.; Zheng, X. *Z. Kristallogr.* **2000**, *215*, 627−631.
(52) Calmuschi, B.; Alesi, M.; Englert, U. *Dalton Trans.* **2004**, 1852−1857.
(53) Fomulu, S. L.; Hendi, M. S.; Davis, R. E.; Wheeler, K. A. *Cryst. Growth Des.* **2002**, *2*, 645−651, 637−644.
(54) Hendi, M. S.; Hooter, P.; Davis, R. E.; Lynch, V. M.; Wheeler, K. A. *Cryst. Growth Des*. **2004**, *4*, 95−101.

CG0506626